

Structurally nonrigid molecular complexes $(\text{HF})_n(\text{H}_2\text{O})_m$ ($n + m \geq 2$) and their spectroscopic features

N. A. Zvereva,^a Sh. Sh. Nabiev,^b Yu. N. Ponomarev,^c and L. P. Sukhanov^{b*}

^aTomsk State University,
36 prospr. Lenina, 634050 Tomsk, Russian Federation.
Fax: +7 (382 2) 23 3034. E-mail: zvereva@phys.tsu.ru

^bRussian Scientific Center "Kurchatov Institute",
1 pl. I. V. Kurchatova, 123182 Moscow, Russian Federation.
Fax: +7 (095) 194 1994. E-mail: nabiev@imp.kiae.ru, sukhanov@imp.kiae.ru

^cInstitute of Atmospheric Optics, Siberian Branch of the Russian Academy of Sciences,
1 Akademicheskii prospr., 634055 Tomsk, Russian Federation.
Fax: +7 (382 2) 25 9086. E-mail: yupon@asd.iao.ru

The problem of the formation and stability of structurally nonrigid, donor–acceptor molecular complexes is considered. These complexes are formed between the molecules of water and hydrogen fluoride, the latter being the hydrolysis product of the chemical, radiochemical, and metallurgical industrial wastes. Based on the results of *ab initio* quantum-chemical calculations of the potential energy surfaces by the Hartree–Fock–Roothaan method, the equilibrium configurations of the $(\text{H}_2\text{O})_n(\text{HF})_m$ complexes ($n : m = 1 : 1; 1 : 2; 2 : 1; 2 : 2$; and $3 : 3$) were determined. These configurations are necessary for correct interpretation of the IR absorption spectra and for routine remote monitoring of such environmentally hazardous complexes in the Earth atmosphere. The harmonic vibrational frequencies of the $(\text{H}_2\text{O})_n(\text{HF})_m$ complexes ($n + m \geq 2$) were calculated and the interaction energies between the monomers were found. The influence of UV radiation on the $(\text{H}_2\text{O})_n(\text{HF})_m$ complexes ($n = 1–3$) upon the transition from the ground to the lowest excited singlet electronic state was studied. Characteristic spectroscopic features of the $(\text{H}_2\text{O})_n(\text{HF})_m$ complexes were established.

Key words: remote probing, lasers, atmosphere, structural nonrigidity, donor–acceptor molecular complexes, quantum-chemical calculations.

Solving problems of on-line monitoring of the gas and aerosol industrial discharges requires obtaining reliable information on the concentrations and molecular compositions of the discharges in the real-time mode. At present, remote probing methods based on the use of the near and mid-IR lasers are thought to be the most promising for this purpose.¹ Efficient use of these instruments as well as the development of physical foundations of novel probing techniques requires detailed information on the vibrational spectra of the radioactive and toxic discharge components. Chemically active anthropogenic toxicants (fluorides, hydrides, *etc.*) can readily interact with the main molecular atmospheric gases and first of all with water vapor present in the Earth atmosphere in rather large amounts (0.02 to 4 mass.% at low altitude).²

In addition to the products of chemical transformations that can mainly occur involving the species present in relatively high concentrations, the donor–acceptor molecular complexes with the bonding energies varying from several tens of calories to several kilocalories can

form under the atmospheric conditions.^{3,4} The optical activity of such complexes can be rather high. Therefore, they can be responsible for additional radiation loss in the atmosphere in some industrial areas (*e.g.*, in the areas with a large number of chemical, radiochemical, electronic, and metallurgical productions, *etc.*) as well as for variations of the solar flux.⁴ Usually, the gas-phase donor–acceptor complexes are characterized by a number of large-amplitude nuclear motions,^{4–6} which alter their vibrational spectra (and parameters of the spectral components) and cause the appearance of new bands corresponding to intermolecular vibrations. In turn, these factors are responsible for severe difficulties when detecting and estimating the concentrations of the molecular complexes in the Earth atmosphere using modern remote probing techniques.

Earlier,^{3–5} we have studied the spectrochemical aspects of the remote monitoring of accidental discharges on nuclear fuel cycle installations and on some productions that employ volatile fluorine-containing compounds

including strong inorganic fluoro oxidants.^{7,8} Analysis showed that the most toxic and chemically reactive components of the discharge plumes of the above-mentioned productions include UF_6 , SiF_4 , and interhalides like XF_3 and XF_5 ($\text{X} = \text{Cl}, \text{Br}$). At the same time, virtually all stages of hydrolysis of these compounds in the Earth atmosphere involve the formation of HF, which is one of the most environmentally hazardous antropogenic, minor gas component of the Earth atmosphere.⁹

Though the parameters of the HF molecule are well known¹⁰ and are available from virtually all spectroscopic database systems (see, e.g., Ref. 11), their use when solving problems of on-line laser monitoring of atmosphere is not always appropriate. This is due to the possibility for stable, structurally nonrigid complexes of general formula $(\text{HF})_n(\text{H}_2\text{O})_m$ ($n + m \geq 2$) to be formed in the interaction between HF and H_2O .^{3–5,8,12} The rovibrational spectra of such complexes can be appreciably different from those of pure HF and H_2O . The formation conditions of stable and long-lived (in the Earth atmosphere) complexes and the parameters of their absorption spectra, which can be employed in developing novel efficient methods for detecting these environmentally hazardous compounds, have virtually not been studied so far.

The aim of this work was to carry out a quantum-chemical study of the structure, stability, and vibrational spectra of the $(\text{HF})_n(\text{H}_2\text{O})_m$ complexes ($n + m \geq 2$) and of the influence of UV radiation on such complexes on going from the ground to the lowest excited singlet electronic state.

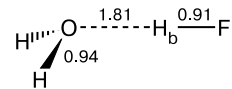


Fig. 1. Geometric parameters of $\text{H}_2\text{O}\dots\text{HF}$ complex (C_s symmetry) obtained from HFR/6-31G** calculations; $E_{\text{tot}} = -176.0497$ au, the $\text{H}\text{—O}\text{—H}$ angle is 107° and the $\text{O}\text{—H}_\text{b}\text{—F}$ angle is 176° . The internuclear distances are given in Å; H_b is the bridging hydrogen atom.

Calculation Procedure

The potential energy surfaces (PES) of the $(\text{HF})_n(\text{H}_2\text{O})_m$ complexes were calculated by the Hartree–Fock–Roothaan (HFR) method using the MONSTERGAUSS¹³ and GAUSSIAN-98¹⁴ program packages which were adapted for personal computers with Pentium® CPUs. The 6-31G** split valence basis set (see, e.g., Ref. 15) employed in this work includes the outer polarization d-functions on the F and O atoms and p-functions on H atoms.

The calculated geometric parameters and energy characteristics of the HF and H_2O molecules and of the $\text{H}_2\text{O}\dots\text{HF}$ complex with C_s symmetry in the configuration corresponding to the absolute minimum on the PES (Fig. 1) are listed in Table 1. The harmonic vibrational frequencies of the monomers and the complex calculated with an increment of ± 0.1 au along the vibrational coordinates are listed in Table 2. For comparison, Tables 1 and 2 also list the experimental values and the results of more precise calculations performed using the Møller–Plesset (MP) perturbation theory with inclusion of electron correlation effects.

As can be seen from the data in Table 1, the calculated equilibrium internuclear distances and the $\text{H}\text{—O}\text{—H}$ bond angle in the monomer molecules differ from the experimental values

Table 1. Geometric parameters and energy characteristics of the HF and H_2O monomers and $\text{H}_2\text{O}\dots\text{HF}$ complex calculated by different methods and corresponding experimental values^a

Molecule	Symmetry	Computational method	ΔE /kcal mol ⁻¹	R_e /Å			Angle/deg		
				$\text{H}_\text{b}\text{—F}$	$\text{O}\text{—H}$	$\text{O}\text{—F}$	$\text{H}\text{—O}\text{—H}$	α	$\text{H}_\text{b}\text{—F}\text{—O}$
HF	$C_{\infty v}$	HFR/6-31G** ^b	—	0.90	—	—	—	—	—
		Experiment ¹⁶	—	0.92	—	—	—	—	—
H_2O	C_{2v}	HFR/6-31G** ^b	—	—	0.94	—	106	—	—
		Experiment ¹⁷	—	—	0.96	—	105	—	—
$\text{H}_2\text{O}\dots\text{HF}$	C_s	HFR/6-31G** ^b	9	0.91	0.94	2.72	107	134	4
		MP2/6-31G** ^b	11	0.93	0.96	2.67	105	131	6
		MP2/6-311G** ¹⁸	11	0.92	0.96 ^c	2.64	105 ^c	129	5
		MP3/6-311G** ¹⁸	11	0.92	0.96 ^c	2.65	105 ^c	133	3
		Experiment ^{18,19}	—	—	—	2.66	—	134	—
		MP4/6-311+G(2d,2p) ²⁰	9 ^d	0.92 ^d	—	2.72 ^d	—	—	5 ^d
		Experiment ²¹	10	—	—	—	—	—	—

^a For the atomic numbering scheme, see Fig. 1; ΔE is the bonding energy of monomers in the complex; and α is the angle between the $\text{O}\text{—F}$ axis and the bisectrix of the $\text{H}\text{—O}\text{—H}$ angle.

^b This work.

^c Calculations¹⁸ at the second- and third-order Møller–Plesset level of perturbation theory (MP2 and MP3, respectively) were carried out with the experimental¹⁷ geometric parameters of the H_2O molecule.

^d Obtained from calculations at the fourth-order Møller–Plesset level of perturbation theory (MP4) performed with the geometric parameters optimized by the HFR/6-31G* method.

Table 2. Harmonic vibrational frequencies (ω_i/cm^{-1}) of the HF and H_2O monomers and $H_2O\cdots HF$ complex

$H_2O\cdots HF$			H_2O			HF		
Calculation ^a	Experiment ²²	Assignment ^b	Calculation ^a	Experiment ¹⁷	Assignment ^b	Calculation	Experiment ¹⁶	Assignment ^b
4270	3608 ± 2	$v(H_bF)$	4265 ^a	3939	$v^{as}(OH)$	4493 ^a	4138	$v(HF)$
4258	3756	$v^{as}(OH)$	4052 ^c	—	—	4212 ^c	—	—
4142	3657	$v^s(OH)$	4010 ^d	—	—	4119 ^d	—	—
1765	1595	$\delta(HOH)$	4148 ^a	3835	$v^s(OH)$	—	—	—
760	696 ± 30	$\delta_i(OH_bF)$	3909 ^c	—	—	—	—	—
626	666 ± 30	$\delta_o(OH_bF)$	3863 ^d	—	—	—	—	—
236	180 ± 30	$v(H_2O\cdots H_bF)$	1770 ^a	1648	$\delta(HOH)$	—	—	—
206	145 ± 50	$\delta_o(HOH_b)$	1674 ^c	—	—	—	—	—
194	170 ± 50	$\delta_i(HOH_b)$	1620 ^d	—	—	—	—	—

^a This work.^b The frequencies (ν)²² of fundamental transitions are reported for the complex (see Fig. 1). Notations: v^s and v^{as} are the symmetrical and asymmetrical stretching vibrations, respectively, and δ denotes the deformation vibrations in plane (δ_i) and out of plane (δ_o) of the H_2O molecule.^c Obtained from our MP2/6-31G** calculations.^d Obtained from MP2/6-31++G** calculations.²³

by at most 0.02 Å and 1°, respectively. The harmonic vibrational frequencies of the monomers (see Table 2) are overestimated (up to 9%) compared to the experimental values. Partial inclusion of electron correlation at the second-order Møller–Plesset (MP2) level of perturbation theory reduces the frequencies and the differences between the calculated and experimental data down to 2%. This agreement between the calculated molecular constants of the monomers and the corresponding experimental values allows the 6-31G** basis set to be used in theoretical studies of the molecular characteristics of the $H_2O\cdots HF$ complex.

Analysis of the data listed in Table 1 and comparison of the results of our calculations of the $H_2O\cdots(HF)_2$ and $HF\cdots(H_2O)_2$ complexes with the corresponding data obtained from more precise MP2 calculations²³ showed that the computational method employed in this work (HFR/6-31G**) for theoretical studies of the $(HF)_n(H_2O)_m$ complexes provides the errors of at most 0.01–0.04 Å for the equilibrium bond lengths in the monomers, 0.05–0.10 Å for the hydrogen bond lengths, 2–10 degrees for the bond angles and dihedral angles, and 1–2 kcal mol⁻¹ for the complexation energies. The harmonic vibrational frequencies (ω_i) of the $H_2O\cdots HF$ complex calculated in this work (see Table 2) are, as a rule, overestimated up to 18 and 42% compared to the experimental frequencies of fundamental transitions (ν_i) corresponding to intramolecular and intermolecular modes, respectively.²² Anharmonicity of the molecular vibrations, which contributes to the frequencies of the fundamental transitions, introduces an additional contribution to an increase in discrepancies with the calculated harmonic frequencies and is significant when describing the vibrational spectra of loosely bound hydrogen-bonded complexes.

The stationary points on the PES of the complexes under study were located using full geometry optimization by the Broiden–Fletcher–Goldfarb–Shanno²⁴ and using a combination of the Newton–Raphson methods.²⁵ Calculations were carried out until a total energy gradient of $5\cdot 10^{-4}$ hartree Bohr⁻¹. This allowed calculations with an accuracy of 0.001 Å for the equilibrium internuclear distances, 3 degrees for the bond angles

and dihedral angles, 0.001 kcal mol⁻¹ for the complexation energies, and ~ 1 cm⁻¹ for harmonic vibrational frequencies. This accuracy of the geometry optimization can be considered reasonable taking into account rather large errors of determination of the parameters of the complexes under study due to incompleteness of the basis set employed and to neglect of electron correlation effects in the HFR computational procedure.

The energies (ϵ) of the $S_0\rightarrow S_1$ vertical electronic transitions were calculated by the restricted Hartree–Fock method for open-shell systems^{26–29} from the total energy differences between the complex in the first excited singlet state, $E_{\text{tot}}(S_1)$, and in the ground singlet state, $E_{\text{tot}}(S_0)$. The excited electronic state S_1 corresponds to transition of an electron from the highest occupied MO, ϕ_{occ} , of the ground state S_0 to the lowest unoccupied MO, ϕ_{vac} , with retention of symmetry of the spin function. The ϵ values calculated for the HF and H_2O monomers (9.7 and 7.8 eV, respectively) are in good agreement with the experimental data³⁰ (10±0.2 and 7.4 eV, respectively). This allowed the use of the computational procedure described above for studying the influence of UV radiation on such complexes in the spectral region corresponding to electronic transitions between the lowest singlet states.

Results and Discussion

The first experimental IR study²² revealed the existence of the $(H_2O)_n(HF)_m$ complexes ($n, m \geq 2$) at high pressures; however, measurements were carried out only for the $H_2O\cdots HF$ (1 : 1) complex. The enthalpy of complex formation, ΔH°_{298} , was estimated at -6.2 kcal mol⁻¹,²² which corresponds to the dissociation energy $D_0 = -5.5$ kcal mol⁻¹ and to the total dissociation energy $D_c = -7.1$ kcal mol⁻¹. Here $|D_c| = |D_0| + \Delta\epsilon_0$, where $\Delta\epsilon_0 = (\epsilon_0(H_2O\cdots HF) - \epsilon_0(H_2O) - \epsilon_0(HF))$ is the zero-point vibrational energy correction for the complex and the

monomers. Further microwave spectroscopy studies^{31–33} of thermodynamically equilibrated $\text{H}_2\text{O}\dots\text{HF}$ gas hydrate ($n(\text{H}_2\text{O}) = 1.85 \cdot 10^{19}$, $n(\text{HF}) = 6.66 \cdot 10^{20}$, $n(\text{H}_2\text{O}\dots\text{HF}) = 10.03 \cdot 10^{15} \text{ m}^{-3}$) showed that the dissociation energy, D_0 , equals $-8.1 \text{ kcal mol}^{-1}$. The estimate of the total dissociation energy ($D_e = -10.2 \text{ kcal mol}^{-1}$) is in good agreement with the results of *ab initio* quantum-chemical calculations²⁰ ($-8.8 \text{ kcal mol}^{-1}$). It should be noted that the latter value is much higher than that obtained from the IR spectra ($-7.1 \text{ kcal mol}^{-1}$),²² whereas the formation enthalpy of the complex obtained from the IR spectroscopic study insignificantly differs from the calculated value²⁰ ($\Delta H^\circ_{298} = -6.2$ and $-7.4 \text{ kcal mol}^{-1}$, respectively).

The IR spectrum of a HF– H_2O mixture in an Ar matrix at 12 K revealed³⁴ the presence of three different types of hydrogen-bonded complexes, namely, $\text{H}_2\text{O}\dots(\text{HF})_2$, $\text{H}_2\text{O}\dots\text{HF}$, and $\text{HF}\dots\text{HOH}$ (listed in the order of increasing stability). Despite the lack of experimental data, the existence of the $(\text{H}_2\text{O})_2\dots\text{HF}$ complex was suggested based on the observation of a strong absorption band in the IR spectrum in the region corresponding to vibrations of the $(\text{H}_2\text{O})_2$ dimer.³⁴

A systematic theoretical study²³ of the structure, stability, and IR spectra of the $\text{H}_2\text{O}\dots(\text{HF})_2$ and $(\text{H}_2\text{O})_2\dots\text{HF}$ complexes allowed the determination of a total of three stable equilibrium structures among all possible configurations of these complexes. However, the existence of the $\text{HF}\dots\text{HOH}$ complex was not established.

In this work we carried out *ab initio* HFR quantum-chemical calculations of the following molecular systems: $\text{H}_2\text{O}\dots\text{HF}$, $\text{H}_2\text{O}\dots(\text{HF})_2$, $(\text{H}_2\text{O})_2\dots\text{HF}$, $(\text{H}_2\text{O}\dots\text{HF})_2$, and $(\text{H}_2\text{O}\dots\text{HF})_3$.

Stability of $(\text{H}_2\text{O})_n(\text{HF})_m$ complexes. The geometry of the $\text{H}_2\text{O}\dots\text{HF}$ complex (C_s symmetry) characterized by a bonding energy, ΔE , of 9 kcal mol^{-1} (see Table 3) and corresponding to the absolute minimum on the PES is shown in Fig. 1. According to our calculations, the energy of the planar structure of this complex with a linear hydrogen bond (C_{2v} symmetry) is $0.05 \text{ kcal mol}^{-1}$ higher (*cf.* $0.13 \text{ kcal mol}^{-1}$ obtained from the HFR calculations¹⁸ with the extended 6-311G** basis set and 0.49 and $0.41 \text{ kcal mol}^{-1}$ according to calculations¹⁸ performed with the same basis set and inclusion of electron correlation by the MP2 method and at the third-order Møller–Plesset (MP3) level of perturbation theory, respectively).

For the $\text{H}_2\text{O}\dots(\text{HF})_2$ complex our calculations predict two stable configurations ($\Delta E = 15$ and 21 kcal mol^{-1} , see Table 3) corresponding to the open and cyclic structures (Fig. 2, *a*, *b*). This is in excellent agreement with the published results.²³ The cyclic configuration of the $\text{H}_2\text{O}\dots(\text{HF})_2$ complex is more stable.

Similarly to the earlier study,²³ the $(\text{H}_2\text{O})_2\dots\text{HF}$ complex corresponds to the cyclic structure (Fig. 2, *c*) with $\Delta E = 20 \text{ kcal mol}^{-1}$ (see Table 3). The cyclic structure of

Table 3. Monomolecular decomposition energies (ΔE) of the $(\text{H}_2\text{O})_n(\text{HF})_m$ complexes, obtained from HFR/6-31G** calculations

Complex	Decomposition products	ΔE /kcal mol ⁻¹
$(\text{H}_2\text{O})(\text{HF})$	$\text{H}_2\text{O} + \text{HF}$	9
$(\text{H}_2\text{O})(\text{HF})_2$	$(\text{H}_2\text{O})(\text{HF}) + \text{HF}$	12
	$\text{H}_2\text{O} + 2 \text{ HF}$	21
$(\text{H}_2\text{O})_2(\text{HF})$	$(\text{H}_2\text{O})(\text{HF}) + \text{H}_2\text{O}$	11
	$2 \text{ H}_2\text{O} + \text{HF}$	20
$(\text{H}_2\text{O})_2(\text{HF})_2$	$(\text{H}_2\text{O})(\text{HF})_2 + \text{H}_2\text{O}$	12
	$(\text{H}_2\text{O})_2(\text{HF}) + \text{HF}$	12
	$2 (\text{H}_2\text{O})(\text{HF})$	15
	$(\text{H}_2\text{O})(\text{HF}) + \text{H}_2\text{O} + \text{HF}$	24
	$2 \text{ H}_2\text{O} + 2 \text{ HF}$	33
$(\text{H}_2\text{O})_3(\text{HF})_3$	$(\text{H}_2\text{O})_2(\text{HF})_2 + (\text{H}_2\text{O})(\text{HF})$	14
	$(\text{H}_2\text{O})_2(\text{HF})_2 + \text{H}_2\text{O} + \text{HF}$	23
	$(\text{H}_2\text{O})_2(\text{HF}) + (\text{H}_2\text{O})(\text{HF})_2$	14
	$(\text{H}_2\text{O})_2(\text{HF}) + (\text{H}_2\text{O})(\text{HF}) + \text{HF}$	26
	$(\text{H}_2\text{O})_2(\text{HF}) + \text{H}_2\text{O} + 2 \text{ HF}$	35
	$(\text{H}_2\text{O})(\text{HF})_2 + (\text{H}_2\text{O})(\text{HF}) + \text{H}_2\text{O}$	25
	$(\text{H}_2\text{O})(\text{HF})_2 + 2 \text{ H}_2\text{O} + \text{HF}$	34
	$3 (\text{H}_2\text{O})(\text{HF})$	28
	$2 (\text{H}_2\text{O})(\text{HF}) + \text{H}_2\text{O} + \text{HF}$	37
	$(\text{H}_2\text{O})(\text{HF}) + 2 \text{ H}_2\text{O} + 2 \text{ HF}$	46
	$3 \text{ H}_2\text{O} + 3 \text{ HF}$	55

Note. The energy, ΔE , of the decomposition reaction $A \rightarrow \sum_i A_i$ is given by the formula $\Delta E = \sum_i E_{\text{tot}}(A_i) - E_{\text{tot}}(A)$, where $E_{\text{tot}}(A)$ and $E_{\text{tot}}(A_i)$ are the total energies of the complex, A , and the decomposition products, A_i , in the lowest energy configurations; $E_{\text{tot}}(\text{H}_2\text{O}) = -76.0236 \text{ au}$ and $E_{\text{tot}}(\text{HF}) = -100.0117 \text{ au}$. For the total energies of other molecular systems, see Notes to Figs. 1–5.

the $(\text{H}_2\text{O})_2(\text{HF})_2$ complex (Fig. 3) is characterized by $\Delta E = 33 \text{ kcal mol}^{-1}$ (see Table 3), while the $(\text{H}_2\text{O})_3(\text{HF})_3$ complex can be formed as both the chain structure with $\Delta E = 36 \text{ kcal mol}^{-1}$ (Fig. 4) and as the cyclic structure with $\Delta E = 55 \text{ kcal mol}^{-1}$ (Fig. 5, see Table 3). Attempts at locating other local minima corresponding to the positive-definite matrix of the second derivatives of the total energy on the PES of the $2 : 1$, $2 : 2$, and $3 : 3$ complexes failed. As follows from Table 3 and Fig. 1–5, the cyclic structure of the $(\text{H}_2\text{O})_3\dots(\text{HF})_3$ complex is the most stable among all configurations of the $(\text{H}_2\text{O})_n(\text{HF})_m$ complexes ($n + m \geq 2$) studied in this work from the standpoint of the bonding energy per H-bond.

More detailed analysis of the data listed in Table 3 showed that all the $(\text{H}_2\text{O})_n(\text{HF})_m$ complexes, except for the chain configuration of the $(\text{H}_2\text{O})_3(\text{HF})_3$ complex (see Fig. 4), are energetically stable toward all types of gas-phase monomolecular decomposition. The chain structure of the $(\text{H}_2\text{O})_3(\text{HF})_3$ complex is unstable toward the decomposition into the $2 : 2$, $1 : 1$, $2 : 1$, and $1 : 2$ complexes. Nevertheless, as will be shown below, this

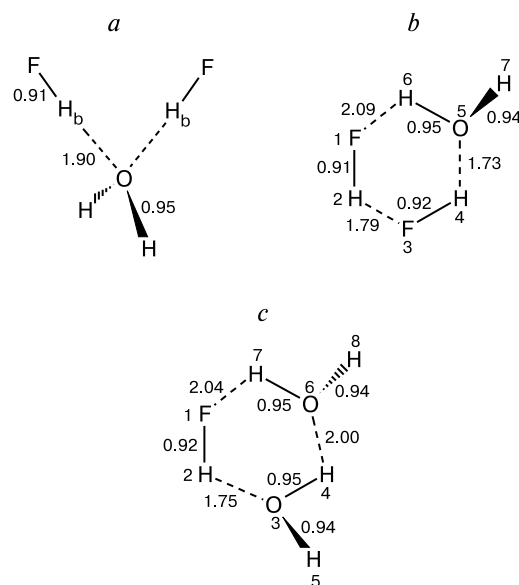


Fig. 2. Geometric parameters of the complexes $H_2O...(HF)_2$ with C_{2v} symmetry (*a*), $H_2O.....(HF)_2$ with C_1 symmetry (*b*), and $(H_2O)_2.....HF$ with C_1 symmetry (*c*), obtained from HFR/6-31G** calculations. The internuclear distances are given in Å. The values of the angles (ω) are listed below.

Complex (symmetry) [- E_{tot} /au]	Angle	ω/deg
$H_2O...(HF)_2$ (C_{2v}) [276.0706]	F—H _b —O	166
	H _b —O—H _b	115
	H—O—H	107
$H_2O.....(HF)_2$ (C_1) [276.0807]	H(6)—O(5)—H(4)	98
	H(2)—F(3)—H(4)	93
	F(3)—H(4)—O(5)	154
	F(1)—H(2)—F(3)	150
	H(6)—O(5)—H(7)	107
	H(4)—O(5)—H(7)	123
	H(4)—F(3)—H(2)—F(1)	-2
	O(5)—H(4)—F(3)—H(2)	0
	H(6)—O(5)—H(4)—F(3)	-3
	H(7)—O(5)—H(4)—F(3)	114
$(H_2O)_2.....HF$ (C_1) [252.0912]	F(1)—H(2)—O(3)	158
	H(2)—O(3)—H(4)	95
	O(3)—H(4)—O(6)	144
	H(7)—O(6)—H(4)	91
	H(2)—O(3)—H(5)	120
	H(8)—O(6)—H(4)	124
	H(5)—O(3)—H(4)	107
	H(7)—O(6)—H(8)	107
	H(4)—O(3)—H(2)—F(1)	-4
	O(6)—H(4)—O(3)—H(2)	5
	H(8)—O(6)—H(4)—O(3)	-113
	H(5)—O(3)—H(2)—F(1)	109
	H(7)—O(6)—H(4)—O(3)	-2

configuration also corresponds to a minimum on the PES and the harmonic force constant matrix is positive-definite in the vicinity of this point. It should also be noted

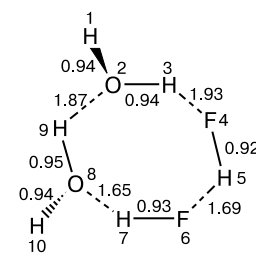


Fig. 3. Geometry of $(H_2O...HF)_2$ complex with C_1 symmetry calculated by the HFR/6-31G** method; $E_{\text{tot}} = -352.1227$ au. The internuclear distances are given in Å. The values of the angles (ω) are listed below.

Angle	ω/deg	Angle	ω/deg
H(1)—O(2)—H(3)	108	H(1)—O(2)—H(3)—F(4)	115
H(9)—O(8)—H(10)	110	H(5)—F(4)—H(3)—O(2)	15
O(2)—H(3)—F(4)	161	F(6)—H(5)—F(4)—H(3)	1
F(4)—H(5)—F(6)	167	H(7)—F(6)—H(5)—F(4)	0
F(6)—H(7)—O(8)	166	O(8)—H(7)—F(6)—H(5)	1
H(3)—F(4)—H(5)	106	H(9)—O(8)—H(7)—F(6)	-6
H(5)—F(6)—H(7)	106	H(10)—O(8)—H(9)—O(2)	-47
H(7)—O(8)—H(9)	116		

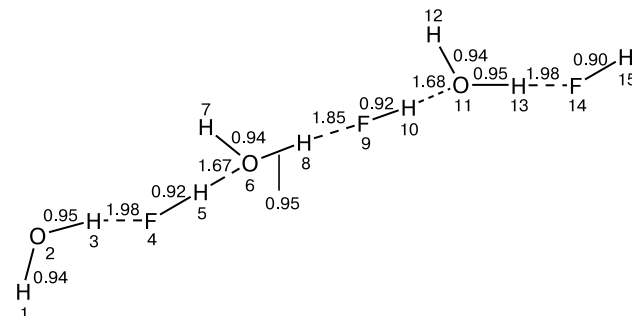


Fig. 4. Geometry of the chain configuration of the $(H_2O...HF)_3$ complex with C_1 symmetry, obtained from HFR/6-31G** calculations; $E_{\text{tot}} = -528.1632$ au. The internuclear distances are given in Å. All torsion angles are equal to 0 and 180°. The values of other angles (ω) are listed below.

Angle	ω/deg	Angle	ω/deg
H(1)—O(2)—H(3)	106	H(8)—F(9)—H(10)	133
O(2)—H(3)—F(4)	169	F(9)—H(10)—O(11)	180
H(3)—F(4)—H(5)	122	H(10)—O(11)—H(12)	129
F(4)—H(5)—O(6)	180	H(12)—O(11)—H(13)	108
H(5)—O(6)—H(7)	127	O(11)—H(13)—F(14)	180
H(7)—O(6)—H(8)	108	H(13)—F(14)—H(15)	140
O(6)—H(8)—F(9)	180		

that the elimination energies of the H_2O and HF monomers from the 1 : 2, 2 : 1, and 2 : 2 complexes virtually coincide, being somewhat higher than the bonding energy in the $H_2O...HF$ heterodimer.

Structural features of some $(H_2O)_n(HF)_n$ complexes. The following trends of changes in the structural param-

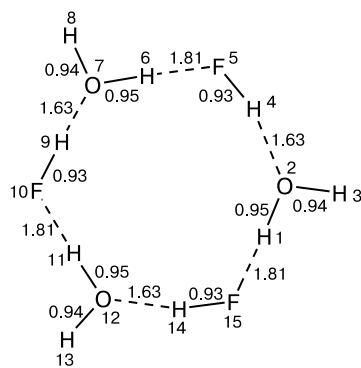


Fig. 5. Geometric parameters of the cyclic configuration of the $(\text{H}_2\text{O}\dots\text{HF})_3$ complex with C_1 symmetry according to HFR/6-31G** calculations; $E_{\text{tot}} = -528.1943$ au. The inter-nuclear distances are given in Å. All torsion angles are equal to 0 and 180° . The values of other angles (ω) are listed below.

Angle	ω/deg	Angle	ω/deg
$\text{H}(1)\text{--O}(2)\text{--H}(3)$	108	$\text{F}(10)\text{--H}(9)\text{--O}(7)$	178
$\text{H}(4)\text{--O}(2)\text{--H}(3)$	126	$\text{H}(11)\text{--F}(10)\text{--H}(9)$	116
$\text{F}(5)\text{--H}(4)\text{--O}(2)$	177	$\text{O}(12)\text{--H}(11)\text{--F}(10)$	179
$\text{H}(6)\text{--F}(5)\text{--H}(4)$	116	$\text{H}(13)\text{--O}(12)\text{--H}(11)$	108
$\text{O}(7)\text{--H}(6)\text{--F}(5)$	178	$\text{H}(14)\text{--O}(12)\text{--H}(13)$	126
$\text{H}(8)\text{--O}(7)\text{--H}(6)$	108	$\text{F}(15)\text{--H}(14)\text{--O}(12)$	177
$\text{H}(9)\text{--O}(7)\text{--H}(8)$	126		

eters of the $(\text{H}_2\text{O})_n(\text{HF})_n$ complexes ($n = 1\text{--}3$) can be pointed out. The $\text{H}_b\text{--F}$ bond is lengthened by 0.01 Å ($n = 1$) and by 0.02–0.03 Å ($n = 2, 3$) compared to the equilibrium bond length in free HF molecule (see Table 1, Figs. 1, 3–5). The like H-bonds ($\text{O}\dots\text{H}_b$) are 0.16 Å ($n = 2$) and 0.13–0.18 Å ($n = 3$) shorter than in the $\text{H}_2\text{O}\dots\text{HF}$ complex. A feature of the cyclic structure ($n = 2$) is appreciable deviation of the $\text{F}\text{--H}_b\text{...O}$ angle from 180° (by 14°) whereas this parameter for the $\text{H}_2\text{O}\dots\text{HF}$ complex is $\sim 4^\circ$. The $\text{F}\text{--H}_b\text{...O}$ angle is 180° in the chain structure of the complex with $n = 3$ while differs from this value only by $2\text{--}3^\circ$ in the cyclic structure. In all complexes the O–H bond involving the terminal H atom of the H_2O molecule has the same length (0.94 Å). The maximum elongation of the bridging O–H_b bond compared to its analog in free H_2O molecule is 0.01 Å ($n = 2, 3$).

Vibrational spectra of $(\text{H}_2\text{O})_n(\text{HF})_m$ complexes. As mentioned above, the harmonic vibrational frequencies (ω_i) calculated in this work differ (sometimes appreciably) from the corresponding experimental frequencies (v_i) of fundamental vibrational transitions. These discrepancies are due to both the errors of the HFR method when calculating the ω_i values and to the large anharmonicity contribution to the vibrational frequencies of H-bonded complexes. An efficient model has been proposed and theoretically substantiated,³⁵ which provides a rather accurate and simple procedure for the inclusion of the con-

tribution of the anharmonicity corrections to the stretching vibration frequencies (v_i) of the Y monomer which forms a $\text{H}_2\text{O}\dots\text{Y}$ complex with a quasi-linear hydrogen bond in the Earth atmosphere. In this work, the vibrational frequencies were corrected using the linear calibration function

$$v_{\text{corr}} = b\omega_{\text{calc}} + a, \quad (1)$$

where ω_{calc} and v_{corr} are the calculated harmonic and corrected vibrational frequencies, respectively, and a and b are the calibration coefficients that can be found by the least-squares method using the experimental²² and calculated data for the $\text{H}_2\text{O}\dots\text{HF}$ complex. The coefficients b and a were found to be 0.84 and 108 cm^{-1} , respectively, while the correlation coefficient between the experimental and calculated frequencies was 0.998.

Table 4 lists the experimental and calculated vibrational frequencies used in the fitting of the a and b coefficients and corresponding to intramolecular modes of the $\text{H}_2\text{O}\dots\text{HF}$ complex (see Fig. 1). The mean absolute deviation of v_{corr} from v_{exp} was 58 cm^{-1} . The harmonic vibrational frequencies of the HF molecule and the HF fragment of the $\text{H}_2\text{O}\dots\text{HF}$ complex obtained from HFR calculations differ by 223 cm^{-1} (see Table 2, cf. a value of 351 cm^{-1} obtained from the experimental^{16,22} frequencies). Thus, calculations in the HFR/6-31G** approximation underestimate the shift of the vibrational frequency of the HF monomer upon the formation of the $\text{F}\text{--H}\dots\text{O}$ hydrogen bond by 130 cm^{-1} . A complete set of the vibrational frequencies of the $\text{H}_2\text{O}\dots\text{HF}$ complex is listed in Table 2.

In Table 5 we present the calculated intramolecular frequencies ω_i and $v_{i,\text{corr}}$ and the results of MP2 calculations²³ of the $\text{H}_2\text{O}\dots(\text{HF})_2$ and $(\text{H}_2\text{O})_2\dots\text{HF}$ complexes. Given for the cyclic structure of the $\text{H}_2\text{O}\dots(\text{HF})_2$ complex are also the results of study,³⁶ the authors of which used a semiempirical model in the method of the F–G matrix using the experimental data. The vibrational frequencies $v_{i,\text{corr}}$ obtained in this work are in reasonable agreement with the results of the earlier study³⁶ and of the IR spectroscopic study³⁴ of a HF– H_2O mixture in the low-temperature Ar matrix. The vibrational frequencies corresponding to the intermolecular modes of the $(\text{H}_2\text{O})_n(\text{HF})_m$ complexes ($n : m = 2 : 1; 1 : 2$) are listed in

Table 4. Experimental²² (v_{exp}) and calculated intramolecular vibrational frequencies (cm^{-1}) of $\text{H}_2\text{O}\dots\text{HF}$ complex (see Fig. 1)

ω_{calc}	v_{exp}^{22}	v_{corr}	Assignment*
4270	3608	3695	$\text{v}(\text{H}_b\text{F})$
4258	3756	3685	$\text{v}^{\text{as}}(\text{OH})$
4142	3657	3587	$\text{v}^{\text{s}}(\text{OH})$
1765	1595	1591	$\delta(\text{HOH})$

Note. For notations of vibrations, see note^b to Table 2.

Table 5. Intramolecular vibrational frequencies (cm^{-1}) of the $\text{H}_2\text{O} \dots (\text{HF})_2$ complex with the chain (see Fig. 2, *a*) and cyclic (see Fig. 2, *b*) structures and those of the $(\text{H}_2\text{O})_2 \dots \text{HF}$ complex (see Fig. 2, *c*)

Complex (symmetry)	ω_i		$\nu_{i,\text{corr}}^a$	Assignment
	I ^b	II ^c		
$(\text{H}_2\text{O}) \cdot (\text{HF})_2$ (C_{2v})	1765 (121)	1636 (98)	1591	$\delta(\text{HOH})$ (A_1)
	4120 (81)	3820 (160)	3567	$\nu(\text{OH})$ (A_1)
	4230 (152)	3851 (1066)	3661	$\nu(\text{OH})$ (B_1)
	4331 (839)	3897 (229)	3746	$\nu(\text{H}_b\text{F})$ (B_2)
	4357 (142)	3957 (144)	3768	$\nu(\text{H}_b\text{F})$ (A_1)
	1777 (112)	1646 (89)	1601	$\delta(\text{H}_6\text{O}_5\text{H}_7)$
$(\text{H}_2\text{O}) \cdot (\text{HF})_2$ (C_1)	4024 (555)	3374 (1111)	3488 [3329, 3272] ^d	$\nu(\text{H}_4\text{F}_3)$
	4103 (190)	3807 (168)	3555 [3590] ^d	$\nu(\text{O}_5\text{H}_6)$
	4228 (154)	3823 (465)	3660 [3715] ^d	$\nu(\text{O}_5\text{H}_7)$
	4268 (544)	3969 (154)	3693 [3703, 3690] ^d	$\nu(\text{H}_2\text{F}_1)$
	1785 (142)	1640 (154)	1607	$\delta(\text{HOH})$
	1788 (77)	1653 (21)	1610	$\delta(\text{HOH})$
$(\text{H}_2\text{O})_2 \cdot \text{HF}$ (C_1)	4018 (166)	3440 (1001)	3483	$\nu(\text{HF})$
	4084 (494)	3703 (345)	3539	$\nu(\text{HO})$
	4115 (385)	3805 (117)	3565	$\nu(\text{HO})$
	4229 (122)	3954 (129)	3660	$\nu(\text{HO})$
	4239 (143)	3974 (126)	3669	$\nu(\text{HO})$

^a Listed are the frequencies of fundamental vibrational transitions corrected using formula (1).

^b This work; listed are the harmonic frequencies, ω_i , and the transition intensities in the IR spectra (in km mol^{-1}) calculated by the HFR/6-31G** method (figures in parentheses).

^c Harmonic frequencies, ω_i , and transition intensities in the IR spectra (in km mol^{-1}) obtained from MP2/6-31++G** calculations²³ (figures in parentheses).

^d Given in square brackets are the vibrational frequency obtained in the framework of the semiempirical model³⁶ using the F—G matrix method followed by the frequency found in the IR spectroscopic study³⁴ of a HF— H_2O mixture in Ar matrix at 12 K.

Table 6. Intermolecular harmonic vibrational frequencies (ω_i) of $\text{H}_2\text{O} \cdot (\text{HF})_2$ and $(\text{H}_2\text{O})_2 \cdot \text{HF}$ complexes

Complex (symmetry)	ω_i/cm^{-1}		Complex (symmetry)	ω_i/cm^{-1}	
	I ^a	II ^b		I ^a	II ^b
$\text{H}_2\text{O} \cdot (\text{HF})_2$ (C_{2v})	691 (65)	782 (390)	$\text{H}_2\text{O} \cdot (\text{HF})_2$ (C_1)	266 (6)	275 (15)
	690 (349)	753 (0)		236 (103)	218 (94)
	647 (238)	712 (253)		223 (7)	209 (4)
	592 (362)	653 (296)		162 (11)	111 (17)
	250 (114)	314 (85)		1017 (115)	1077 (162)
	199 (23)	231 (0)		805 (359)	903 (274)
	175 (0)	212 (1)		644 (264)	658 (249)
	167 (3)	184 (0)		544 (322)	500 (189)
	100 (0)	144 (1)		374 (72)	388 (72)
	32 (12)	33 (10)		299 (13)	326 (69)
$\text{H}_2\text{O} \cdot (\text{HF})_2$ (C_1)	1055 (121)	1117 (144)		260 (90)	293 (111)
	805 (409)	902 (300)		258 (5)	266 (5)
	669 (378)	654 (344)		202 (2)	215 (11)
	548 (91)	583 (99)		175 (188)	196 (164)
	522 (240)	477 (204)		159 (8)	127 (11)
	334 (60)	355 (82)			

^a See note^b to Table 5.

^b See note^c to Table 5.

Table 6. The vibrational frequencies corresponding to the intra- and intermolecular modes of the $(\text{H}_2\text{O} \dots \text{HF})_2$ com-

plex calculated in this work are listed in Tables 7 and 8, respectively.

Table 7. Intramolecular vibrational frequencies (in cm^{-1}) of $(\text{H}_2\text{O})_2\cdots(\text{HF})_2$ complex (see Fig. 3)

ω_i^a	$\nu_{i,\text{corr}}^b$	Assignment
1764 (147)	1590	$\delta(\text{HOH})$
1776 (62)	1600	$\delta(\text{HOH})$
3844 (1038)	3337	$\nu(\text{HF})$
4009 (422)	3476	$\nu(\text{HO})$
4139 (526)	3585	$\nu(\text{HF})$
4171 (385)	3612	$\nu(\text{HO})$
4256 (50)	3683	$\nu(\text{HO})$
4263 (38)	3689	$\nu(\text{HO})$

^a See note^b to Table 5.^b See note^a to Table 5.**Table 8.** Intermolecular harmonic vibrational frequencies (ω_i/cm^{-1}) of the $(\text{H}_2\text{O})_2\cdots(\text{HF})_2$ and $(\text{H}_2\text{O})_3\cdots(\text{HF})_3$ complexes in the chain and cyclic configurations and the band intensities in the IR spectra ($A/\text{km mol}^{-1}$), obtained from HFR/6-31G** calculations

Complex (symmetry, configuration)	ω_i	A	Complex (symmetry, configuration)	ω_i	A
$(\text{H}_2\text{O})_2\cdots(\text{HF})_2$ (C_1)	39	56	$(\text{H}_2\text{O})_3\cdots(\text{HF})_3$ (C_1 , chain configuration, see Fig. 4)	411	0
	52	51		471	27
	99	70		479	174
	162	106		653	90
	185	1		687	127
	214	9		717	455
	240	18		916	259
	249	76		956	184
	293	27	$(\text{H}_2\text{O})_3\cdots(\text{HF})_3$ (C_1 , cyclic configuration, see Fig. 5)	30	0
	408	83		30	0
	491	137		39	3
	636	77		51	4
	728	97		51	4
	762	400		104	0
	853	341		147	0
	1099	215		199	44
$(\text{H}_2\text{O})_3\cdots(\text{HF})_3$ (C_1 , chain configuration, see Fig. 4)	12	10		200	44
	19	6		229	450
	20	1		240	0
	23	2		240	0
	43	0		308	4
	74	3		308	4
	86	13		339	0
	115	308		386	0
	128	1		447	46
	154	21		448	47
	168	147		518	0
	193	109		518	0
	222	170		548	356
	247	105		751	0
	277	11		751	0
	306	3		777	778
	347	39		1003	199
	370	145		1003	299
	402	52		1003	0

Table 9. Intramolecular vibrational frequencies (in cm^{-1}) of the chain configuration of $(\text{H}_2\text{O})_3\cdots(\text{HF})_3$ complex (see Fig. 4)

ω_i^a	$\nu_{i,\text{corr}}^b$	Assignment
1779 (87)	1602	$\delta(\text{HOH})$
1804 (204)	1623	$\delta(\text{HOH})$
1811 (6)	1629	$\delta(\text{HOH})$
3919 (1012)	3400	$\nu(\text{HO})$
4006 (1180)	3473	$\nu(\text{HF})$
4012 (586)	3478	$\nu(\text{HF})$
4123 (137)	3571	$\nu(\text{HO})$
4144 (129)	3589	$\nu(\text{HO})$
4256 (98)	3683	$\nu(\text{HO})$
4266 (102)	3691	$\nu(\text{HO})$
4274 (213)	3698	$\nu(\text{HO})$
4453 (209)	3849	$\nu(\text{HF})$

^a See note^b to Table 5.^b See note^a to Table 5.**Table 10.** Intramolecular vibrational frequencies (in cm^{-1}) of the cyclic configuration of $(\text{H}_2\text{O})_3\cdots(\text{HF})_3$ complex (see Fig. 5)

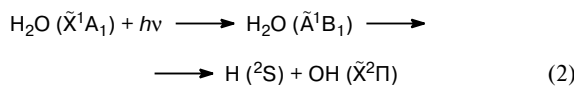
ω_i^a	$\nu_{i,\text{corr}}^b$	Assignment
1802 (146)	1622	$\delta(\text{HOH})$
1802 (145)	1622	$\delta(\text{HOH})$
1810 (0)	1628	$\delta(\text{HOH})$
3829 (0)	3324	$\nu(\text{HF})$
3889 (2291)	3375	$\nu(\text{HF})$
3889 (2291)	3375	$\nu(\text{HF})$
4074 (345)	3530	$\nu(\text{HO})$
4074 (346)	3530	$\nu(\text{HO})$
4077 (0)	3533	$\nu(\text{OH})$
4262 (211)	3688	$\nu(\text{OH})$
4261 (212)	3687	$\nu(\text{OH})$
4262 (1)	3688	$\nu(\text{OH})$

^a See note^b to Table 5.^b See note^a to Table 5.

Analysis of the data presented in Tables 2, 4, 5, 7, 9, and 10 revealed an appreciable low-frequency shift of the stretching vibration frequencies of the HF monomer upon the formation of hydrogen-bonded complexes $(\text{H}_2\text{O})_n(\text{HF})_m$. This shift varies from 223 cm^{-1} for the heterodimer up to 664 cm^{-1} for the cyclic configuration of the $(\text{H}_2\text{O}\cdots\text{HF})_3$ complex (see Table 10).

Electronic transitions between the lowest singlet states of $(\text{H}_2\text{O})_n(\text{HF})_n$ complexes. Analysis of the electron density redistribution on the atoms of the complexes under study upon the $S_0 \rightarrow S_1$ electronic excitation showed that the excitation is, as a rule, localized on one of the water molecules constituting a particular complex. The shape of the cross-section of the PES along the $R(\text{O}-\text{H})$ coordinate in the H_2O molecule on which the excitation is localized clearly indicates the dissociation character of the

$E(S_1)$ electronic term.⁵ The photodissociation character of the \tilde{A}^1B_1 state corresponding to the first absorption band of the water monomer ($\lambda \approx 165$ nm) is well known.^{30,37}



The complexes under study exhibit a Rydberg character of the S_1 electronic state (as in the case of water monomer). The $S_0 \rightarrow S_1$ electronic transition can be described as a $\pi \rightarrow \sigma^*$ ($[2p_z](\text{O}) \rightarrow [3s, 3p_y](\text{O})$) transition.

According to our calculations, one can expect a high-frequency shift of maxima of the absorption bands of the complexes under study relative to the absorption band of the water monomer upon the $S_0 \rightarrow S_1$ electronic transition (Fig. 6). For the $\text{H}_2\text{O} \dots \text{HF}$ complex, this shift is $\Delta\nu_e^{\text{el}} = \epsilon(\text{H}_2\text{O} \dots \text{HF}) - \epsilon(\text{H}_2\text{O}) = 8.57 \text{ eV} - 7.80 \text{ eV} = 0.77 \text{ eV}$ (ϵ is the energy of the corresponding vertical electronic transition). Among the $(\text{H}_2\text{O})_n \dots (\text{HF})_m$ complexes with $n = m = 1 \dots 3$, the largest frequency shift $\Delta\nu_e^{\text{el}}$ (1.20 eV) is expected for the cyclic structure of the $(\text{H}_2\text{O})_3 \dots (\text{HF})_3$ complex. The $\Delta\nu_e^{\text{el}}$ parameters for the chain configuration of the $(\text{H}_2\text{O})_3 \dots (\text{HF})_3$ complex and the cyclic structure of the $(\text{H}_2\text{O})_2 \dots (\text{HF})_2$ complex are 0.84 and 1.06 eV, respectively.

The vertical ionization potentials (IPs) for all complexes calculated in this work from the differences between the total energies of the molecular systems lie in the range 12.8–13.6 eV and are close to that calculated for the H_2O monomer (12.6 eV), which virtually coincides with the experimental value (see, e.g., Ref. 38). Close values of the IPs of the complexes and monomer indicate that ionization of the complexes usually leads to detachment of an electron from one of the water molecules in the complexes. The energies of the electronic transitions to the continuous spectrum are 4–5 eV higher than those of the $S_0 \rightarrow S_1$ electronic excitations.

Thus, in addition to the previously studied $(\text{H}_2\text{O})_n \dots (\text{HF})_m$ complexes ($n : m = 1 : 1, 1 : 2$, and $2 : 1$), in this work we studied the complexes with $n : m = 2 : 2$ and $3 : 3$, which allowed us to obtain valuable information required for correct interpretation of the IR and UV spectra of a mixture of water vapor with HF under the atmospheric conditions. Using the same computational approach, we revealed some trends of formation of the en-

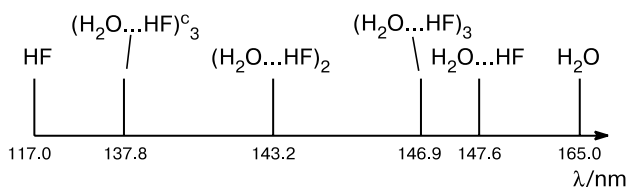


Fig. 6. Positions of the UV absorption band maxima of $(\text{H}_2\text{O} \dots \text{HF})_n$ complexes in the spectral region corresponding to electronic transitions between the lowest singlet states.

ergy, structural, and spectroscopic characteristics of the above-mentioned complexes with an increase in the number of the monomer molecules.

With respect to the intermolecular interaction energy per H-bond the cyclic structure of the $(\text{H}_2\text{O})_3 \dots (\text{HF})_3$ complex is the most stable among all stable configurations of the $(\text{H}_2\text{O})_n (\text{HF})_m$ complexes ($n + m \geq 2$) studied in this work. According to our calculations, the cyclic configurations of the $(\text{H}_2\text{O})_n (\text{HF})_m$ complexes (at least, at $n + m \leq 6$) are more energetically favorable than other structures including the open-chain structures. Analogous results were obtained for both the $(\text{H}_2\text{O})_n$ complexes (see, e.g., Refs. 39 and 40), and the $(\text{HF})_n$ clusters (see, e.g., Ref. 41) at $n \leq 6$.

Among the vibrational frequencies corresponding to intramolecular modes of the complexes studied, the stretching vibration frequency of HF is changed to the greatest extent upon complexation. For all the complexes, the $\nu(\text{HF})$ frequency experiences a low frequency shift. The second group of low-frequency vibrations corresponds to intermolecular modes of the $(\text{H}_2\text{O} \dots \text{HF})_n$ complexes and falls in the frequency range from nearly 10 to 1100 cm^{-1} .

The $S_0 \rightarrow S_1$ electronic excitation in the $(\text{H}_2\text{O} \dots \text{HF})_n$ complexes is localized on the O–H bond of one of the H_2O molecules. Similarly to the H_2O molecule, the complexes also exhibit a Rydberg character of the $S_0 \rightarrow S_1$ transition and the photodissociation type of the corresponding absorption band. Intermolecular interactions in the $(\text{H}_2\text{O} \dots \text{HF})_n$ complexes ($n = 1 \dots 3$) cause a shift of the absorption band maxima toward the short-wavelength region (similarly to the $(\text{H}_2\text{O})_n$ clusters with $n = 2 \dots 6$)^{42,43} compared to the corresponding bands in the water monomer spectrum. These shifts are 0.77 eV ($n = 1$), 1.06 eV ($n = 2$, cyclic structure), 0.84 eV ($n = 3$, chain structure), and 1.20 eV ($n = 3$, cyclic structure).

This work was carried out with the financial support of the Russian Foundation for Basic Research (Project No. 00-05-64919).

References

1. V. E. Zuev, Yu. S. Makushkin, and Yu. N. Ponomarev, *Sovremennye problemy atmosfernoi optiki. 3. Spektroskopiya atmosfery* [Modern Problems of Atmospheric Optics. Atmospheric Spectroscopy], Gidrometeoizdat, Leningrad, 1987, 247 pp. (in Russian).
2. J. Heichlen, *Atmospheric Chemistry*, Academic Press, New York, 1976, 412 pp.
3. Sh. Sh. Nabiev and Yu. N. Ponomarev, *Optika Atmosfery i Okeana* [Atmospheric and Ocean Optics], 1998, **11**, 1274 (in Russian).
4. Sh. Sh. Nabiev, P. G. Sennikov, and Yu. N. Ponomarev, *Abstrs. 8th Colloq. "Atmospheric Spectroscopy Applications"*, Reims, France, 1999, CP2.

5. N. A. Zvereva, Sh. Sh. Nabiev, and Yu. N. Ponomarev, *Optika Atmosfery i Okeana* [Atmospheric and Ocean Optics], 1999, **12**, 843 (in Russian).
6. Sh. Sh. Nabiev and L. P. Sukhanov, *Izv. Akad. Nauk, Ser. Khim.*, 1999, 1415 [*Russ. Chem. Bull.*, 1999, **48**, 1397 (Engl. Transl.)].
7. Sh. Sh. Nabiev, *Optika Atmosfery i Okeana* [Atmospheric and Ocean Optics], 2000, **13**, 123 (in Russian).
8. Sh. Sh. Nabiev, A. N. Trotsenko, S. K. Ignatov, P. G. Sennikov, N. A. Zvereva, and Yu. N. Ponomarev, *Tez. Dokl. Mezhdunar. Simp. "Atmosfernaya Radiatsiya"* [Abstrs. Int. Symp. on Atmospheric Radiation], Izd-vo SPbGU, Sankt-Peterburg, 1999, 127 (in Russian).
9. K. Wark and C. F. Warner, *Air Pollution. Its Origin and Control*, Harper and Row, New York, 1976.
10. K. Nakamoto, *Infrared and Raman Spectra of Inorganic and Coordination Compounds*, Wiley, New York—Chichester—Toronto, 1986.
11. N. Husson, B. Bonnett, N. Scott, and A. Chedin, *J. Quant. Spectrosc. Radiat. Transfer*, 1992, **48**, 509.
12. N. A. Zvereva, Sh. Sh. Nabiev, and Yu. N. Ponomarev, *Proc. SPIE*, 1999, **3983**, 9.
13. M. Peterson and R. Poirier, *MONSTERGAUSS-90*, University of Toronto and Memorial University of Newfoundland, St. John's Newfoundland, 1990.
14. M. J. Frisch, G. W. Trucks, H. B. Schlegel, G. E. Scuseria, M. A. Robb, J. R. Cheeseman, V. G. Zakrzewski, J. A. Montgomery, Jr., R. E. Stratmann, J. C. Burant, S. Dapprich, J. M. Millam, A. D. Daniels, K. N. Kudin, M. C. Strain, O. Farkas, J. Tomasi, V. Barone, M. Cossi, R. Cammi, B. Mennucci, C. Pomelli, C. Adamo, S. Clifford, J. Ochterski, G. A. Petersson, P. Y. Ayala, Q. Cui, K. Morokuma, D. K. Malick, A. D. Rabuck, K. Raghavachari, J. B. Foresman, J. Cioslowski, J. V. Ortiz, B. B. Stefanov, G. Liu, A. Liashenko, P. Piskorz, I. Komaromi, R. Gomperts, R. L. Martin, D. J. Fox, T. Keith, M. A. Al-Laham, C. Y. Peng, A. Nanayakkara, C. Gonzalez, M. Challacombe, P. M. W. Gill, B. G. Johnson, W. Chen, M. W. Wong, J. L. Andres, M. Head-Gordon, E. S. Replogle, and J. A. Pople, *GAUSSIAN-98, Revision A.3*, Gaussian, Inc., Pittsburgh (PA), 1998.
15. T. Clark, *A Handbook of Computational Chemistry*, Wiley, New York, 1985.
16. K. P. Huber and G. Herzberg, *Constants of Diatomic Molecules*, Van Nostrand Reinhold, Toronto, 1979.
17. *Molekulyarnye postoyannye neorganicheskikh soedinenii* [Molecular Constants of Inorganic Compounds]: A Handbook, Ed. K. S. Krasnov, Khimiya, Leningrad, 1979, 448 pp. (in Russian).
18. M. M. Szczesniak, S. Scheiner, and Y. Bouteiller, *J. Chem. Phys.*, 1984, **81**, 5024.
19. J. W. Bevan, Z. Kisiel, A. C. Legon, D. J. Millen, and S. C. Rogers, *Proc. R. Soc. London, Ser. A*, 1980, **372**, 441.
20. J. E. Del Bene, *J. Phys. Chem.*, 1988, **92**, 2874.
21. S. L. A. Adebayo, A. C. Legon, and D. J. Millen, *J. Chem. Soc., Faraday Trans.*, 1991, **87**, 443.
22. R. K. Thomas, *Proc. R. Soc. London, Ser. A*, 1975, **344**, 579.
23. C. Rovira, P. Constants, M. H. Whangbo, and J. J. Novoa, *Int. J. Quant. Chem.*, 1994, **52**, 177.
24. R. Fletcher, *Comput. J.*, 1970, **13**, 317.
25. M. J. D. Powell, *Numerical Methods for Nonlinear Algebraic Equations*, Gordon and Breach, London, 1970, 87.
26. C. C. J. Roothaan, *Rev. Mod. Phys.*, 1960, **32**, 179.
27. K. Hirao and H. Nakatsui, *J. Chem. Phys.*, 1973, **59**, 1457.
28. K. Hirao, *J. Chem. Phys.*, 1974, **60**, 3215.
29. R. Carbo and J. M. Riera, *Lecture Notes in Chemistry. 5. A General SCF Theory*, Springer, Berlin, 1978.
30. A. M. Pravilov, *Fotoprotsessy v molekulyarnykh gazakh* [Photoprocesses in Molecular Gases], Energoatomizdat, Moscow, 1992, 350 pp. (in Russian).
31. A. C. Legon, D. J. Millen, and H. M. North, *Chem. Phys. Lett.*, 1987, **135**, 303.
32. G. Gazzoli, P. G. Favero, D. G. Lister, A. C. Legon, D. J. Millen, and Z. Kisiel, *Chem. Phys. Lett.*, 1985, **117**, 543.
33. S. P. Belov, V. M. Demkin, N. F. Zobov, E. N. Karyakin, A. F. Krupnov, I. N. Kozin, O. L. Polyanskii, and M. Yu. Tret'yakov, *Prepr. IPF Akad. Nauk SSSR* [Prepr. Int. Appl. Phys., USSR Acad. Sci.] No. 192, Gor'kii, 1988, 17 pp. (in Russian).
34. L. Andrews and G. L. Johnson, *J. Chem. Phys.*, 1983, **79**, 3670.
35. L. P. Sukhanov, V. V. Zheleznyakov, and N. L. Zakamskaya, *Zh. Fiz. Khim.*, 2001, **75**, 1972 [*Russ. J. Phys. Chem.*, 2001, **75**, 1808 (Engl. Transl.)].
36. E. G. Tarakanova, F. Huisken, and M. Kaloudis, *Proc. SPIE*, 1997, **3090**, 180.
37. T. G. Meister, *Elektronnye spektry mnogoatomnykh molekul* [Electronic Spectra of Polyatomic Molecules], Izd-vo LGU, Leningrad, 1969, 206 pp. (in Russian).
38. W. R. Wadt and W. A. Goddard, *Chem. Phys.*, 1976, **18**, 1.
39. S. S. Xantheas and T. H. Dunning, Jr., *J. Chem. Phys.*, 1993, **99**, 8774.
40. S. S. Xantheas, *J. Chem. Phys.*, 1995, **102**, 4505.
41. F. Huisken, E. G. Tarakanova, A. A. Vigasin, and G. V. Yukhnevich, *Chem. Phys. Lett.*, 1995, **245**, 319.
42. N. A. Zvereva, M. A. Buldakov, I. I. Ippolitov, and A. F. Terpugova, *Izv. Vuz. Fiz.*, 1993, **36**, 11 [*Bull. Vuz. Physics*, 1980 (Engl. Transl.)].
43. N. A. Zvereva and I. I. Ippolitov, *Proc. SPIE*, 1997, **3090**, 88.

Received August 31, 2001,
in revised form May 22, 2002